

Underestimated passive volcanic sulfur degassing implies overestimated anthropogenic aerosol forcing

3 U. A. Jongebloed¹, A. J. Schauer², J. Cole-Dai³, C. G. Lerrick³, R. Wood¹, T. P. Fischer⁴, S.
 4 A. Carn⁵, S. Salimi¹, S. R. Edouard², S. Zhai¹, L. Geng⁶, and B. Alexander¹

⁵ ¹ Department of Atmospheric Sciences, University of Washington, Seattle, WA, USA

⁶ ² Department of Earth and Space Sciences, University of Washington, Seattle, WA, USA

7 ³ Department of Chemistry and Biochemistry, South Dakota State University, Brookings, SD,
8 USA

9 ⁴ Department of Earth and Planetary Sciences, University of New Mexico, Albuquerque, NM,
10 USA

5 Department of Geological and Mining Engineering and Sciences, Michigan Technological
12 University, Houghton, MI, USA

⁶ School of Earth and Space Sciences, University of Science and Technology of China, Hefei, Anhui, China

15 Corresponding author: Becky Alexander (beckya@uw.edu)

16 Key Points:

- Sulfur isotopes in a Greenland ice core show that passive volcanic degassing contributes 66% of preindustrial Arctic sulfate
- The volcanic inventory used by most climate models underestimates passive degassing, possibly due to missing hydrogen sulfide emissions
- Elevated preindustrial passive volcanic degassing reduces the estimated cooling effect of anthropogenic sulfate in the Arctic

23 Abstract

24 The Arctic is warming at almost four times the global rate. Cooling caused by anthropogenic
25 aerosols has been estimated to offset sixty percent of greenhouse-gas-induced Arctic warming,
26 but the contribution of aerosols to radiative forcing (RF) represents the largest uncertainty in
27 estimating total RF, largely due to unknown preindustrial aerosol abundance. Here, sulfur
28 isotope measurements in a Greenland ice core show that passive volcanic degassing contributes
29 up to $66 \pm 10\%$ of preindustrial ice core sulfate in years without major eruptions. A state-of-the-
30 art model indicates passive volcanic sulfur emissions influencing the Arctic are underestimated
31 by up to a factor of three, possibly because many volcanic inventories do not include hydrogen
32 sulfide emissions. Higher preindustrial volcanic sulfur emissions reduce modeled anthropogenic
33 Arctic aerosol cooling by up to a factor of two ($+0.11$ to $+0.29 \text{ W m}^{-2}$), suggesting that
34 underestimating passive volcanic sulfur emissions has significant implications for
35 anthropogenic-induced Arctic climate change.

36 Plain Language Summary

37 Sulfate aerosols are particles in the atmosphere that have a net cooling effect on the climate. One
38 of the most uncertain aspects of climate modeling is the abundance of sulfate aerosols during the
39 preindustrial era. Without knowing the amount of sulfate aerosols during the preindustrial, it is
40 difficult to estimate how much anthropogenic sulfate aerosols have offset warming from
41 anthropogenic greenhouse gases. In this study, we examine preindustrial sulfate aerosols in a
42 Greenland ice core. We find that sulfate aerosols from passive (i.e. non-eruptive) volcanic
43 degassing contribute almost two thirds of preindustrial Arctic sulfate aerosols in years without
44 major volcanic eruptions. We compare this result to a state-of-the-art global model and find that
45 most climate models use a volcanic emissions inventory that underestimates preindustrial passive
46 volcanic sulfur emissions. That volcanic inventory only includes one type of sulfur emission
47 (sulfur dioxide), but studies have shown that volcanoes emit hydrogen sulfide, which can also
48 form sulfate aerosols. We show that higher emissions of volcanic sulfur during the preindustrial
49 era decrease the estimated cooling effect of anthropogenic aerosols during the industrial era.
50 Thus, the underestimate of preindustrial volcanic emissions in current climate models has
51 significant implications for anthropogenic climate change in the Arctic.

52 1 Introduction

53 Anthropogenic aerosols have a net cooling effect on global climate and partially offset
54 warming from greenhouse gases, but represent the largest uncertainty in estimating total
55 anthropogenic radiative forcing (RF) from 1850-2019 (Szopa et al., 2021). Aerosol RF results
56 from aerosol-radiation interactions (RF_{ari}), including scattering solar radiation (Twomey, 1967),
57 and aerosol-cloud interactions (RF_{aci}), including changing cloud albedo (Twomey, 1977). Other
58 aerosol effects such as impacts on cloud fraction and lifetime are uncertain, but may be
59 significant in the Arctic (Shindell et al., 2013). Sulfate aerosols have the largest cooling effect of
60 any aerosol and their contribution to RF also has the largest uncertainty (Szopa et al., 2021).

61 The magnitude of aerosol RF depends on preindustrial aerosol abundance due to the
62 nonlinear relationship between aerosols and cloud albedo: as aerosol abundance increases, cloud
63 sensitivity to aerosol decreases. Thus, one of the largest sources of uncertainty in aerosol RF is
64 poorly constrained natural emissions of aerosol precursors (Carslaw et al., 2013; Gettelman,

65 2015), especially emissions of volcanic sulfur dioxide (SO_2) and marine dimethyl sulfide (DMS),
 66 which are dominant natural sources of Arctic sulfate aerosol (Abbatt et al., 2019; Legrand et al.,
 67 1997; Patris et al., 2002; Wasiuta et al., 2006). Other potential sources of sulfate aerosol,
 68 including carbonyl sulfide, dust, and biomass burning, are negligible in the Arctic (Abbatt et al.,
 69 2019; Kjellström, 1998; Legrand et al., 1997; Patris et al., 2002; Wasiuta et al., 2006). Although
 70 volcanic eruptions garner more attention in the climate literature, passive emissions of SO_2 are
 71 currently estimated to be about ten times the typical annual emissions of SO_2 from eruptions
 72 (Carn et al., 2017).

73 Satellites provide global daily observations of volcanic SO_2 emissions from eruptive and
 74 passive degassing (Carn et al., 2015, 2017). Ground-based observations show that these satellite
 75 observations provide a lower-end estimate on volcanic SO_2 emissions because satellite detection
 76 limits are too high to reliably detect passive emissions from weakly degassing volcanoes (Fischer
 77 et al., 2019). Furthermore, volcanic SO_2 emissions inventories are primarily derived from UV
 78 satellite measurements, which have data gaps at high latitudes in the winter months (Carn et al.,
 79 2017). In addition to underestimating SO_2 emissions, these inventories exclude emissions of
 80 other sulfur species such as hydrogen sulfide (H_2S), which is difficult to measure from space due
 81 to a lack of characteristic absorption bands in the near UV and an overlap of IR absorption bands
 82 with those of water vapor (Clarisso et al., 2011). Estimates of volcanic H_2S emissions range from
 83 1 to 35 Tg S yr^{-1} (Halmer et al., 2002); the upper end of this range is three times the estimated
 84 global annual mean eruptive plus passive volcanic SO_2 flux of 11-13 Tg S yr^{-1} (Carn et al., 2015,
 85 2017). After emission, H_2S is oxidized to SO_2 on the timescale of 1-3 days (D'Alessandro et al.,
 86 2009; Kourtidis et al., 2008; Pham et al., 1995), by which point it is too dispersed to be detected
 87 by satellite. Thus, satellite observations underestimate volcanic sulfur emissions (Carn et al.,
 88 2017; Fischer et al., 2019), but the magnitude of the underestimate and the contribution of
 89 volcanic sulfur to the global sulfur burden remains unquantified.

90 2 Quantifying preindustrial sources of ice core sulfate

91 We quantify volcanic and DMS-derived biogenic contribution to preindustrial (1200 to 1850
 92 C.E.) Arctic sulfate aerosols by measuring sulfate concentrations (SO_4^{2-}) and sulfur isotopic
 93 composition ($\delta^{34}\text{S}(\text{SO}_4^{2-})$) in ice core samples from Summit, Greenland (see Text S1 for details
 94 on measurement methods). We select samples from years without influence from large volcanic
 95 eruptions (Figure 1, Cole-Dai et al., 2013; Gautier et al., 2019).

96 To estimate the relative contribution of volcanic and DMS-derived biogenic sulfate to total
 97 ice core non-sea salt sulfate (nssSO_4^{2-}), we assume that $\delta^{34}\text{S}(\text{nssSO}_4^{2-})$ is a concentration-
 98 weighted average of the mean biogenic sulfate isotopic composition ($\delta^{34}\text{S}_{\text{bio}}$) and mean volcanic
 99 sulfate isotopic composition ($\delta^{34}\text{S}_{\text{volc}}$):

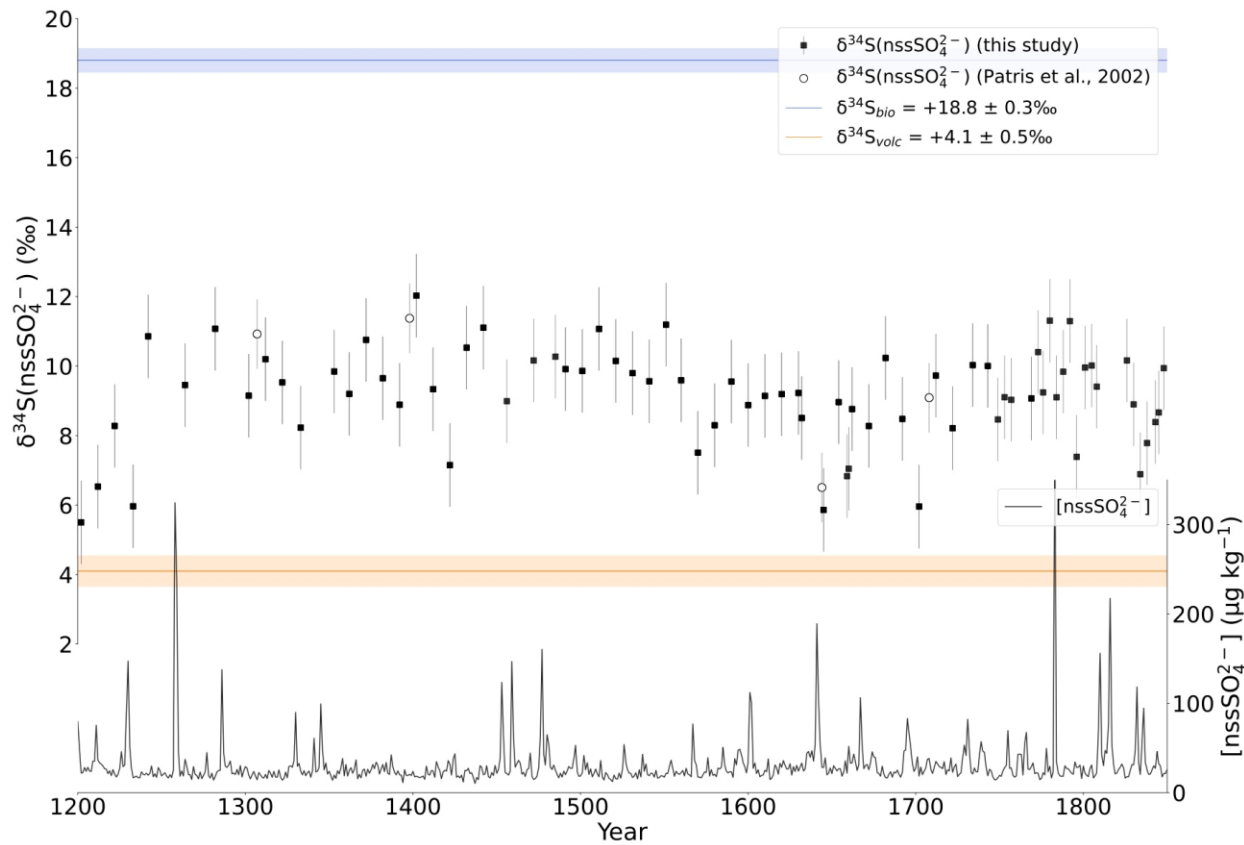
$$100 \quad f_{\text{bio}} + f_{\text{volc}} = 1, \text{ and} \\ 101 \quad f_{\text{bio}} \delta^{34}\text{S}_{\text{bio}} + f_{\text{volc}} \delta^{34}\text{S}_{\text{volc}} = \delta^{34}\text{S}(\text{nssSO}_4^{2-}),$$

102 where f_{bio} is the fraction of DMS-derived biogenic sulfate and f_{volc} is the fraction of volcanic
 103 sulfate. $\delta^{34}\text{S}_{\text{bio}}$ is well constrained by measurements of sulfur isotopic composition of marine
 104 biogenic compounds at $\delta^{34}\text{S}_{\text{bio}} = +18.8 \pm 0.3\text{\textperthousand}$ (Table S1 and Figure S1). Observations of sulfate
 105 from an inland Antarctic ice core far from the marine biogenic source show $\delta^{34}\text{S}_{\text{bio}} = +18.6 \pm$
 106 $0.9\text{\textperthousand}$ (Patris et al., 2000), suggesting minimal fractionation due to transport and oxidation of
 107 marine biogenic sulfur (Text S2).

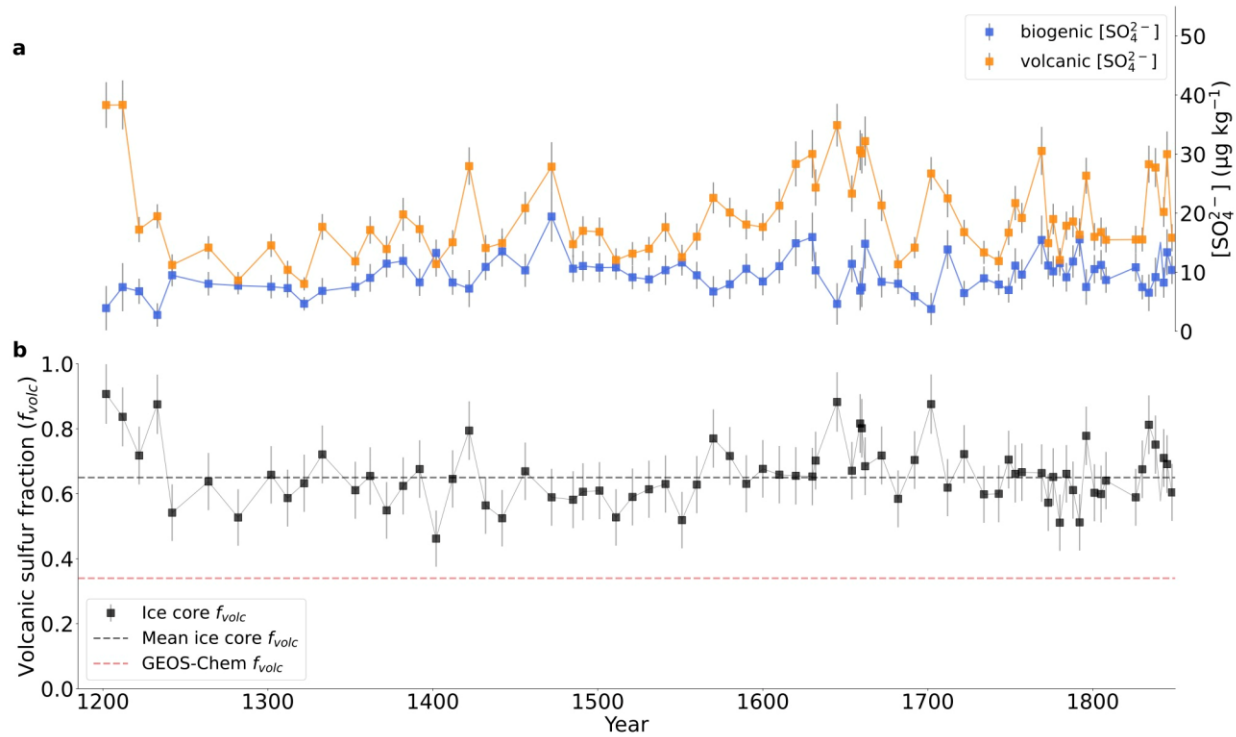
108 We estimate $\delta^{34}\text{S}_{\text{volc}}$ using two methods. First, we estimate $\delta^{34}\text{S}_{\text{volc}}$ by applying a Monte
 109 Carlo routine to a Keeling Plot (Keeling, 1958; Keeling et al., 1989; Pataki et al., 2003) of the ice

110 core observations to determine $\delta^{34}\text{S}_{\text{volc}} = +4.1 \pm 0.5 \text{‰}$ (Figure S2 and Table S3) using similar
 111 assumptions and methods as in Patris et al. (2000, 2002) (Text S2). Second, we use direct $\delta^{34}\text{S}$
 112 observations of volcanic gas and ash from 367 measurements of volcanic $\delta^{34}\text{S}(\text{H}_2\text{S})$, $\delta^{34}\text{S}(\text{SO}_4^{2-})$,
 113 $\delta^{34}\text{S}(\text{SO}_2)$, and $\delta^{34}\text{S}(\text{bulk S})$ from 38 volcanoes around the world (Table S2) to yield $\delta^{34}\text{S}_{\text{volc}} =$
 114 $+3.8 \pm 0.7 \text{‰}$, where the standard error of the mean is determined using a bootstrapping method
 115 (Figure S1 and Text S2). Both estimates of $\delta^{34}\text{S}_{\text{volc}}$ ($+4.1 \pm 0.5 \text{‰}$ and $+3.8 \pm 0.7 \text{‰}$) result in
 116 similar values for mean ice core f_{volc} (66% and 64%, respectively; Text S3), but we focus on
 117 $\delta^{34}\text{S}_{\text{volc}} = +4.1 \pm 0.5 \text{‰}$ because this value more likely represents a regional signature and also
 118 incorporates any fractionation effects on $\delta^{34}\text{S}_{\text{volc}}$ during transport to Summit.

119 Figure 1 shows ice core $\delta^{34}\text{S}(\text{nssSO}_4^{2-})$ and nssSO_4^{2-} concentration between 1200 and 1850
 120 C.E. The mean $\delta^{34}\text{S}(\text{nssSO}_4^{2-})$ is $+9.2 \text{‰}$, indicating that the isotopically lighter volcanic sulfur
 121 contributes about twice as much on average as the biogenic sulfur source. Figure 2 shows that
 122 the mean volcanic sulfate concentration ($19.1 \pm 7.1 \text{ }\mu\text{g kg}^{-1}$) is 2.0 ± 1.7 times larger than the
 123 mean DMS-derived biogenic sulfate concentration ($9.4 \pm 3.0 \text{ }\mu\text{g kg}^{-1}$) and that the mean fraction
 124 of sulfate from volcanoes (f_{volc}) is $66 \pm 10\%$. Using $\delta^{34}\text{S}_{\text{volc}} = +2.5 \text{‰}$ from a small number of
 125 observations from volcanoes near Greenland also yields a dominant contribution from volcanic
 126 sulfate ($f_{\text{volc}} = 59\%$) (Text S3). We also consider how our estimate for f_{volc} is affected by
 127 including a continental source of sulfur (e.g. H_2S emissions from vegetation, salt marshes,
 128 tropical forests, soils, and wetlands) based on Watts (2000), which results in $f_{\text{volc}} = 58$ to 60%
 129 (Text S4). These numbers are similar to a previous estimate of $f_{\text{volc}} = 57\%$ from Legrand et al.
 130 (1997) in a Summit, Greenland ice core, which was estimated by subtracting an assumed DMS-
 131 derived contribution to ice core sulfate based on the summertime peak in nssSO_4^{2-} .



133 **Figure 1.** Decadal and sub-decadal ice core $\delta^{34}\text{S}(\text{nssSO}_4^{2-})$ (‰, black symbols) and annual mean
 134 nss SO_4^{2-} concentration ($\mu\text{g kg}^{-1}$, gray line). Thick colored bars show the isotopic signatures of
 135 volcanic sulfur ($\delta^{34}\text{S}_{\text{volc}} = +4.1 \pm 0.5 \text{ ‰}$) and DMS-derived biogenic sulfur ($\delta^{34}\text{S}_{\text{bio}} = +18.8 \pm 0.3$
 136 ‰). The $\delta^{34}\text{S}(\text{nssSO}_4^{2-})$ samples were selected as one 2-year sample per decade from 1200-1750
 137 C.E. and one 1-year sample every four years from 1750-1850 C.E. from years where nss SO_4^{2-}
 138 was not influenced by large tropospheric or stratospheric eruptions (Cole-Dai et al., 2013;
 139 Gautier et al., 2019). Data from Patris et al. (2002) is also shown (circle). Error in $\delta^{34}\text{S}(\text{nssSO}_4^{2-})$
 140 measurements is estimated based on replicate analysis of whole-process standards.
 141



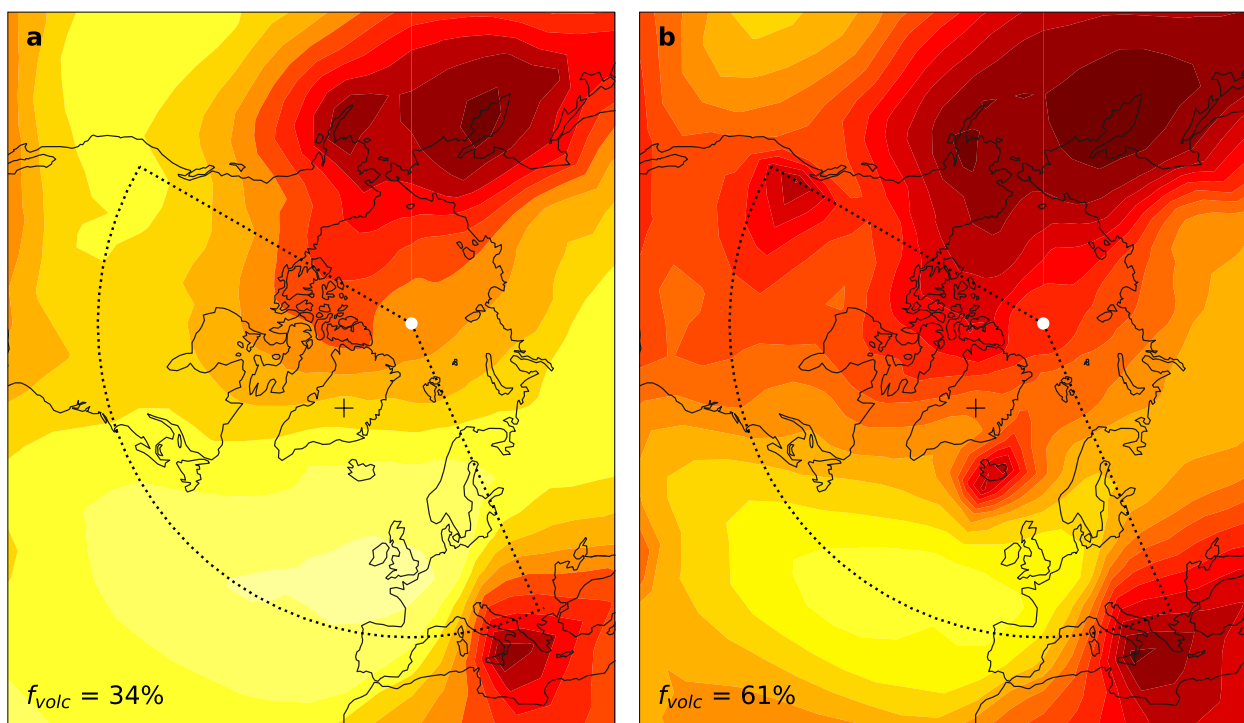
142 **Figure 2.** Volcanic and DMS-derived biogenic sulfate concentrations and volcanic fraction in ice
 143 core samples from preindustrial years (1200-1850 C.E.) without large volcanic eruptions. **(a)**
 144 Volcanic (orange) and DMS-derived biogenic (blue) sulfate concentrations ($\mu\text{g kg}^{-1}$) calculated
 145 with $\delta^{34}\text{S}_{\text{volc}} = +4.1 \pm 0.5 \text{ ‰}$. **(b)** Volcanic fraction of ice core nss SO_4^{2-} in each sample during the
 146 preindustrial (1200 to 1850 C.E.). Dashed gray line shows the mean volcanic fraction of ice core
 147 nss SO_4^{2-} ($f_{\text{volc}} = 66\%$). Dashed red line shows the GEOS-Chem simulated volcanic sulfur fraction
 148 ($f_{\text{volc}} = 34\%$) in the air-mass source region of Summit with the default volcanic SO_2 emissions
 149 from Carn et al. (2015, 2017). Error bars were determined by propagating the uncertainty in
 150 isotopic source signatures and sample measurement error in both a and b.
 151

152 **3 Comparing ice core sulfate to a global model**

153 To evaluate current estimates of the relative importance of volcanic and DMS-derived
 154 biogenic sulfate aerosol abundance in global models, we use the GEOS-Chem global 3-D
 155 chemical transport model (version 13.2.1, Text S5) described in Bey et al. (2001) driven by
 156 assimilated meteorology from MERRA-2. Volcanic SO_2 emissions are from Carn et al. (2015,

157 2017), updated annually in (Carn, 2022). The Carn et al. (2015, 2017) SO₂ emissions inventory is
 158 used in many global models and is the upper end of volcanic SO₂ emissions in Climate Model
 159 Intercomparison Project (CMIP6) models. The Carn et al. (2015, 2017) inventory includes
 160 passive and eruptive volcanic SO₂ emissions measured by the Ozone Monitoring Instrument
 161 (OMI) since 2005. Model DMS emissions are based on Lana et al. (2011). To simulate a
 162 preindustrial atmosphere, all anthropogenic emissions are turned off (Zhai et al., 2021). We use
 163 meteorology and volcanic SO₂ emissions from the year 2013, during which passive and eruptive
 164 volcanic SO₂ emissions in regions affecting the Arctic (i.e., Kamchatka, Alaska, and Iceland)
 165 were similar to the 2004–2017 median. To compare model results to ice-core derived estimate of
 166 f_{volc} , the average f_{volc} of the modeled tropospheric burden of SO₂ and sulfate is computed in the
 167 Summit, Greenland air-mass source region (120°W–30°E, 42°–90°N) based on the 5-day
 168 average aerosol lifetime in the Arctic and HYSPLIT backward trajectory analysis (Zhai et al.,
 169 2021). The modeled f_{volc} is similar when calculated with other methods, including f_{volc} of
 170 modeled sulfur deposition in the ice core region (Figure S3), and when modeled with
 171 meteorology from the year 2007 (Text S5).

172 Figure 3a shows that the modeled preindustrial f_{volc} over the Summit, Greenland air-mass
 173 source region using the SO₂ emissions reported by Carn et al. (2015, 2017) is 34%, which is 3.2
 174 standard deviations lower than the mean ice core f_{volc} . The modeled volcanic sulfur contribution
 175 ($f_{volc} = 34\%$) is lower than the observed f_{volc} in all 74 ice core samples representing 123 years
 176 between 1200 and 1850 C.E. (Figure 2b).
 177



178
 179 **Figure 3.** Modeled tropospheric f_{volc} in two preindustrial simulations. **(a)** Tropospheric f_{volc} in the
 180 preindustrial simulation with the default scenario volcanic emissions. **(b)** Tropospheric f_{volc} in the
 181 preindustrial simulation with emissions from the H₂S 1.7 scenario. Dotted black lines outline the
 182 5-day back trajectory region (120°W–30°E, 42°–90°N) for the Summit, Greenland ice core

183 (location marked with “+”) as described in Zhai et al. (2021). The mean f_{volc} of the sulfur ($\text{SO}_2 +$
184 SO_4^{2-}) burden for the air-mass source region are shown in the bottom left.

185 **4 Discussion**

186 **4.1 Biogenic and continental sulfur emissions and chemistry**

187 A model underestimate in f_{volc} relative to the ice-core derived estimate f_{volc} could be explained
188 by an overestimate in modeled DMS emissions or an underestimate in modeled volcanic
189 emissions. Modeled preindustrial DMS emissions would have to be overestimated by a factor of
190 three for DMS emissions to explain the model underestimate in f_{volc} . Ice core records show
191 declining concentrations of methanesulfonic acid, an oxidation product of DMS, since the
192 preindustrial (Osman et al., 2019), indicating that it is unlikely that present-day DMS flux is
193 three times higher than that of the preindustrial. It is also unlikely that DMS emissions in the
194 Arctic are overestimated by a factor of three; in fact, GEOS-Chem modeled atmospheric DMS
195 concentrations are biased low in the Arctic (Text S6; Mungall et al., 2016). Although modeled
196 DMS oxidation chemistry is simplified, uncertainty in modeled DMS chemistry cannot explain
197 the discrepancy between modeled and observed f_{volc} (Text S6).

198 It is possible that other sources of sulfur not considered in global climate models could
199 contribute to Arctic sulfate. For example, continental emissions of H_2S (e.g. vegetation, salt
200 marshes, tropical forests, soils, and wetlands) contribute approximately 1.5 Tg S yr^{-1} globally
201 (Watts, 2000). However, even if we assume this source contributes up to 4% of ice core sulfate,
202 thereby lowering ice core f_{volc} to 58-60% from 66% (Text S4), the model would still
203 underestimate f_{volc} in the Summit, Greenland back trajectory region.

204 **4.2 Underestimate in passive volcanic degassing emissions**

205 Given the low likelihood of an overestimation of DMS-derived sulfate in the Arctic, the
206 discrepancy between modeled and ice core f_{volc} is best explained by an underestimate in passive
207 volcanic sulfur emissions, which is consistent with comparisons between satellite and ground-
208 based observations of SO_2 (Fischer et al., 2019) and the omission of volcanic H_2S emissions in
209 models. It is also possible that preindustrial passive volcanic degassing was elevated relative to
210 the present day. The sampled time period (1200-1850 C.E.) is during the “Little Ice Age” (LIA),
211 usually defined as a period of relatively cool climate starting in the mid-thirteenth century and
212 ending around 1850 C.E. (Grove, 2001). A driving factor in cooling observed during the LIA
213 was an increased frequency of volcanic eruptions (Newhall et al., 2018). It is conceivable that
214 passive volcanic degassing, which increases prior to and following volcanic eruptions (Carn et
215 al., 2017), was also elevated during the preindustrial relative to the present day, which would
216 exacerbate the underestimate in passive sulfur degassing emissions in the preindustrial. Elevated
217 passive sulfur degassing around periods of increased eruption frequency has been suggested to
218 explain differences between early and late 19th-century $\delta^{34}\text{S}(\text{nssSO}_4^{2-})$ in Antarctic ice cores
219 (Takahashi et al., 2022).

220 To quantify and understand the factors contributing to the underestimate in preindustrial
221 volcanic emissions, three volcanic emissions scenarios were prescribed in the model in place of
222 the Carn et al. (2015, 2017) inventory: we label them the 371 scenario, the H_2S scenario, and the
223 H_2S 1.7 scenario (summarized in Table S4). These emissions scenarios have increased passive

224 degassing of SO₂ relative to Carn et al. (2015, 2017) while leaving eruptive emissions
 225 unchanged. In the 371 scenario, volcanic SO₂ emissions are based on comparison between
 226 satellite and ground-based passive volcanic sulfur emissions from Fischer et al (2019) for
 227 volcanoes included in the Carn et al. (2015, 2017) SO₂ inventory. The 371 scenario also includes
 228 SO₂ fluxes from the 371 volcanoes identified as degassing by Fischer et al. (2019) that are not
 229 included in the Carn et al. (2015, 2017) SO₂ inventory. These 371 volcanoes are classified as
 230 either “hydrothermal” or “magmatic” and fluxes are assigned to be 3 or 7 t S day⁻¹ (0.001 or
 231 0.003 Tg S year⁻¹), respectively (Fischer et al., 2019). This includes 16 Icelandic volcanoes each
 232 emitting 3 t S day⁻¹ (0.017 Tg S year⁻¹ in total). The 371 scenario results in a modest increase in
 233 f_{volc} in the Greenland air mass region from 34% in the default scenario to 36%, still three
 234 standard deviations below the mean ice core f_{volc} of 66% (Figure 2b).

235 In the H₂S scenario, we hypothesize that preindustrial and present-day simulations are
 236 missing a significant volcanic sulfur source due to the omission of H₂S from volcanic emissions
 237 inventories. Here, H₂S contribution is represented by increasing modeled SO₂ emissions due to
 238 the short 1- to 3-day lifetime of H₂S against oxidation to SO₂ (D’Alessandro et al., 2009;
 239 Kourtidis et al., 2008; Pham et al., 1995). Accordingly, SO₂ emissions are multiplied by a factor
 240 based on measured or predicted SO₂ to H₂S ratios (Halmer et al., 2002; Table S5). The H₂S
 241 scenario results in a f_{volc} of 46%, which is 2 standard deviations below the mean ice core f_{volc} of
 242 66%.

243 In the H₂S 1.7 scenario, we multiply the SO₂ emissions from the H₂S scenario by 1.7 for each
 244 volcano. We choose the factor of 1.7 to approximate the mean ice core f_{volc} of 66%. As expected
 245 and shown in Fig. 3b, the H₂S 1.7 scenario produces f_{volc} of 61%, which approximately aligns
 246 with the mean ice core f_{volc} of 66%. This scenario implies that current estimates of preindustrial
 247 volcanic emissions are underestimated due to the omission of H₂S emissions and/or that passive
 248 volcanic degassing has decreased since the preindustrial.

249 We also consider a scenario where only Icelandic volcanoes have increased sulfur emissions
 250 and that these emissions are much larger than Icelandic emissions in the three aforementioned
 251 emissions scenarios (Text S7). SO₂ emissions from Iceland were 5.1 Tg S yr⁻¹ in this scenario,
 252 which is 30 times larger than sulfur emissions from Iceland in the H₂S 1.7 scenario (0.16 Tg S yr⁻¹),
 253 but both scenarios are within the estimated range of sulfur emissions from Icelandic volcanoes
 254 based on observations from Icelandic hot springs (Text S7; Supplementary Data File 2).
 255 Icelandic volcanic sulfur emissions of this magnitude reconcile the discrepancy between the
 256 model and ice core (Text S7). Given the recent studies indicating that passive volcanic degassing
 257 CO₂ emissions in Iceland might be significantly underestimated (e.g., Ilyinskaya et al., 2018), it
 258 is possible that underestimated Icelandic volcanic sulfur emissions could explain most or all of
 259 the discrepancy between the ice core and modeled f_{volc} . This possibility also has significant
 260 radiative forcing implications (Text S7), and highlights the large uncertainty and
 261 disproportionate impact of Icelandic volcanic emissions in the North Atlantic and Greenland.

262 4.3 Radiative forcing implications

263 Models indicate that the cooling effect of anthropogenic aerosols would be lower than
 264 previously thought if the preindustrial sulfate aerosol abundance was higher because of the
 265 nonlinear relationship between aerosols and RF_{aci}: as preindustrial aerosol abundance increases,
 266 cloud albedo becomes less sensitive to anthropogenic aerosols (Carslaw et al., 2013; Gettelman
 267 et al., 2015). To explore the potential RF implications of our emissions scenarios, we consider
 268 three possibilities. First, we assume that the default volcanic emissions inventory from Carn et al.

(2015, 2017) accurately estimates present-day emissions, but underestimates passive volcanic sulfur emissions in the preindustrial. Second, we assume that passive volcanic sulfur emissions have not changed since the preindustrial, and that both preindustrial and present-day passive degassing emissions are underestimated. Overlapping volcanic and anthropogenic sulfur isotopic source signatures preclude quantifying volcanic sulfate in post-1850 ice core samples (Ghahremaninezhad et al., 2016; Patris et al., 2002; Wasiuta et al., 2006), therefore we cannot use post-1850 ice core measurements to evaluate this possibility. A third possibility is a combination of the first two: volcanic sulfur emissions in both present-day and preindustrial are underestimated and volcanic passive sulfur emissions were higher in the preindustrial relative to the present day. The RF implications of this third possibility will fall in between the first two.

To quantify the RF implications of an underestimate in passive volcanic degassing emissions in the preindustrial (first possibility) or both the preindustrial and present day (second possibility), we estimate RF for each possibility ($RF = RF_{ari} + RF_{aci}$), where RF_{ari} is calculated using GEOS-Chem (Text S5) and RF_{aci} is calculated using the simple heuristic model described by Wood 2021 (Text S8). We estimate ΔRF by subtracting RF with the Carn et al. (2015, 2017) inventory from RF with elevated passive degassing emissions representing the first or second possibility (Table S6). We quantify ΔRF for the first possibility by using the H_2S 1.7 scenario in the preindustrial and using the default scenario in the present day. We quantify ΔRF for the second possibility by using the H_2S 1.7 scenario in both the preindustrial and present day. We focus on the H_2S 1.7 scenario because it results in a preindustrial modeled f_{volc} (61%) approximately equal to the ice core f_{volc} (66%). The resulting ΔRF for both possibilities are summarized in Table 1. ΔRF ranges from $+0.29 \text{ W m}^{-2}$ ($\Delta RF_{ari} = +0.03 \text{ W m}^{-2}$, $\Delta RF_{aci} = +0.26 \text{ W m}^{-2}$; Table 1, Figure S4) where only preindustrial emissions are underestimated, to $+0.11 \text{ W m}^{-2}$ ($\Delta RF_{ari} = 0.0 \text{ W m}^{-2}$, $\Delta RF_{aci} = +0.11 \text{ W m}^{-2}$; Table 1, Figure S4) where both preindustrial and present-day emissions are underestimated. We estimate that underestimating Icelandic passive volcanic sulfur emissions could have an equally large or larger impact on radiative forcing ($\Delta RF = +0.55 \text{ W m}^{-2}$) (Text S7). This analysis neglects the effects of cloud adjustments to aerosol (i.e., impacts on cloud fraction, cloud lifetime, and semi-direct aerosol effects). Nevertheless, these calculations show that the impact of underestimating volcanic emissions on RF calculations is potentially large. Future studies using fully coupled atmosphere-ocean global climate models with enhanced volcanic emissions will be useful for more accurately quantifying RF implications and uncertainty.

Table 1. Radiative forcing (RF) estimates for different present-day and preindustrial volcanic scenarios.

Emissions Scenario	Volcanic Emissions Scenario in Present Day (f_{volc} of natural $nssSO_4^{2-}$)	Volcanic Emissions Scenario in Preindustrial (f_{volc} of natural $nssSO_4^{2-}$)	Arctic aerosol SW TOA RF ^a (RF_{ari} ^b + RF_{aci} ^c) between present day and in preindustrial (W m^{-2})	Difference between default Arctic RF and emissions scenario Arctic RF (W m^{-2}) ($\Delta RF_{ari} + \Delta RF_{aci}$)
Default	Default ($f_{volc} = 34\%$)	Default ($f_{volc} = 34\%$)	$-0.55 (-0.10 + -0.45)$	
Possibility 1	Default ($f_{volc} = 34\%$)	H_2S 1.7 ($f_{volc} = 61\%$)	$-0.26 (-0.07 + -0.19)$	$+0.29 (0.03 + 0.26)$
Possibility 2	H_2S 1.7 ($f_{volc} = 61\%$)	H_2S 1.7 ($f_{volc} = 61\%$)	$-0.44 (-0.10 + -0.34)$	$+0.11 (0.00d + 0.11)$

^a The total shortwave (SW) top-of-atmosphere (TOA) radiative forcing (RF) is estimated as the sum of the RF from aerosol-radiation interactions (RF_{ari}) and RF from aerosol-cloud interaction (RF_{aci}).

^b Difference between present-day radiative effect from aerosol-radiation interactions and preindustrial radiative effect from aerosol-radiation interactions.

^c Estimated present-day RF from aerosol-cloud interactions (Text S8).

309 ^d $\Delta\text{RF}_{\text{ari}}$ between the default possibility and possibility 2 is negligible compared to $\Delta\text{RF}_{\text{aci}}$

310 **5 Conclusions**

311 Our results indicate that passive volcanic degassing sulfur emissions influencing the Arctic
312 are underestimated by up to a factor of three. We show that increased volcanic sulfur emissions
313 from passive degassing results in estimated Arctic anthropogenic aerosol cooling that is up to a
314 factor of two lower in magnitude. An overly strong anthropogenic aerosol cooling due to
315 underestimated passive volcanic sulfur degassing could at least partially explain excessively
316 strong aerosol cooling in CMIP6 climate models (Dittus et al., 2020) and the underestimates of
317 modeled Arctic amplification compared to observations (Rantanen et al., 2022).

318 Quantifying passive volcanic sulfur degassing emissions is critical for constraining
319 anthropogenic aerosol forcing. More observations of SO_2 emissions from passive volcanic
320 degassing are required to constrain the magnitude of the underestimate in the passive volcanic
321 SO_2 emissions inventory based on satellite measurements in Carn et al. (2015, 2017).
322 Additionally, H_2S , which is typically neglected in volcanic emissions inventories used in global
323 climate models, should be considered a potentially important contributor to the global
324 atmospheric sulfur budget and thus climate.

325 **Acknowledgments**

326 U.J. and B.A. acknowledge financial support from NSF award numbers PLR 1904128 and
327 AGS 1702266. J.C.-D. is supported by PLR 0612461 and PLR 1904142. R.W. is supported by
328 Lowercarbon, the Pritzker Innovation Fund, and Silver-Lining, through the Marine Cloud
329 Brightening Project. T.F. acknowledges support from the Deep Carbon Observatory, DECADE
330 initiative for work on the global volcanic SO_2 and CO_2 flux inventories. S.C. acknowledges
331 support from NASA Interdisciplinary Research in Earth Science (80NSSC20K1773) and NASA
332 Aura Science Team (80NSSC20K0983). L.G. acknowledges support from National Natural
333 Science Foundation of China (41822605 and 41871051).

334 **Open Research**

335 All ice-core data and Iceland volcanic gas observations are available in the National Science
336 Foundation (NSF) Arctic Data Center at <https://doi.org/10.18739/A2N873162>. GEOS-Chem
337 version 13.2.1 code is publicly available at <https://doi.org/10.5281/zenodo.5500717>.

338 **References**

339 Abbatt, J. P. D., Richard Leaitch, W., Aliabadi, A. A., Bertram, A. K., Blanchet, J. P., Boivin-
340 Rioux, A., et al. (2019). Overview paper: New insights into aerosol and climate in the
341 Arctic. *Atmospheric Chemistry and Physics*, 19(4), 2527–2560. <https://doi.org/10.5194/acp-19-2527-2019>

343 Bey, I., Jacob, D. J., Yantosca, R. M., Logan, J. A., Field, B. D., Fiore, A. M., et al. (2001).
344 Global modeling of tropospheric chemistry with assimilated meteorology: Model
345 description and evaluation. *Journal of Geophysical Research*, 106(D19), 23,073-23,095.
346 <https://doi.org/10.1029/2001JD000807>

347 Carn, S. A., Yang, K., Prata, A. J., & Krotkov, N. A. (2015). Extending the long-term record of
348 volcanic SO₂ emissions with the Ozone Mapping and Profiler Suite nadir mapper.
349 *Geophysical Research Letters*, 42(3), 925–932. <https://doi.org/10.1002/2014GL062437>

350 Carn, S. A., Fioletov, V. E., McLinden, C. A., Li, C., & Krotkov, N. A. (2017). A decade of
351 global volcanic SO₂ emissions measured from space. *Scientific Reports*, 7.
352 <https://doi.org/10.1038/srep44095>

353 Carn, Simon A. (2022). Multi-Satellite Volcanic Sulfur Dioxide L4 Long-Term Global Database
354 V4.

355 Carslaw, K. S., Lee, L. A., Reddington, C. L., Pringle, K. J., Rap, A., Forster, P. M., et al.
356 (2013). Large contribution of natural aerosols to uncertainty in indirect forcing. *Nature*,
357 503(7474), 67–71. <https://doi.org/10.1038/nature12674>

358 Clarisse, L., Coheur, P. F., Chefdeville, S., Lacour, J. L., Hurtmans, D., & Clerbaux, C. (2011).
359 Infrared satellite observations of hydrogen sulfide in the volcanic plume of the August 2008
360 Kasatochi eruption. *Geophysical Research Letters*, 38(10).
361 <https://doi.org/10.1029/2011GL047402>

362 Cole-Dai, J., Ferris, D. G., Lanciki, A. L., Savarino, J., Thiemens, M. H., & McConnell, J. R.
363 (2013). Two likely stratospheric volcanic eruptions in the 1450s C.E. found in a bipolar,
364 subannually dated 800 year ice core record. *Journal of Geophysical Research Atmospheres*,
365 118(14), 7459–7466. <https://doi.org/10.1002/jgrd.50587>

366 D'Alessandro, W., Brusca, L., Kyriakopoulos, K., Michas, G., & Papadakis, G. (2009).
367 Hydrogen sulphide as a natural air contaminant in volcanic/geothermal areas: The case of
368 Sousaki, Corinthia (Greece). *Environmental Geology*, 57(8), 1723–1728.
369 <https://doi.org/10.1007/s00254-008-1453-3>

370 Dittus, A. J., Hawkins, E., Wilcox, L. J., Sutton, R. T., Smith, C. J., Andrews, M. B., & Forster,
371 P. M. (2020). Sensitivity of Historical Climate Simulations to Uncertain Aerosol Forcing.
372 *Geophysical Research Letters*, 47(13). <https://doi.org/10.1029/2019GL085806>

373 Fischer, T. P., Arellano, S., Carn, S., Aiuppa, A., Galle, B., Allard, P., et al. (2019). The
374 emissions of CO₂ and other volatiles from the world's subaerial volcanoes. *Scientific
375 Reports*, 9(1). <https://doi.org/10.1038/s41598-019-54682-1>

376 Gautier, E., Savarino, J., Hoek, J., Erbland, J., Caillon, N., Hattori, S., et al. (2019). 2600-years
377 of stratospheric volcanism through sulfate isotopes. *Nature Communications*, 10(1).
378 <https://doi.org/10.1038/s41467-019-08357-0>

379 Gettelman, A. (2015). Putting the clouds back in aerosol-cloud interactions. *Atmospheric
380 Chemistry and Physics*, 15(21), 12397–12411. <https://doi.org/10.5194/acp-15-12397-2015>

381 Ghahremaninezhad, R., Norman, A. L., Abbatt, J. P. D., Levasseur, M., & Thomas, J. L. (2016).
382 Biogenic, anthropogenic and sea salt sulfate size-segregated aerosols in the Arctic summer.
383 *Atmospheric Chemistry and Physics*, 16(8), 5191–5202. <https://doi.org/10.5194/acp-16-5191-2016>

385 Grove, J. M. (2001). The Onset of the Little Ice Age. In Jones (Ed.), *History and Climate:
386 Memories of the Future?* (pp. 153–185). Dordrecht, Kluwer Academic/Plenum Publishing.

387 Halmer, M. M., Schmincke, H.-U., & Graf, H.-F. (2002). The annual volcanic gas input into the
388 atmosphere, in particular into the stratosphere: a global data set for the past 100 years.
389 *Journal of Volcanology and Geothermal Research*, 115, 511–528.
390 [https://doi.org/10.1016/S0377-0273\(01\)00318-3](https://doi.org/10.1016/S0377-0273(01)00318-3)

391 Ilyinskaya, E., Mobbs, S., Burton, R., Burton, M., Pardini, F., Pfeffer, M. A., et al. (2018).
392 Globally Significant CO₂ Emissions From Katla, a Subglacial Volcano in Iceland.
393 *Geophysical Research Letters*, 45(19). <https://doi.org/10.1029/2018GL079096>

394 Keeling, C. D. (1958). The concentration and isotopic abundances of atmospheric carbon dioxide
395 in rural areas. *Geochimica et Cosmochimica Acta*, 13, 322. [https://doi.org/10.1016/0016-7037\(58\)90033-4](https://doi.org/10.1016/0016-7037(58)90033-4)

396 Keeling, C. D., Bacastow, R. B., Carter, A. F., Piper, S. C., Whorf, T. P., Heimann, M., et al.
397 (1989). A three-dimensional model of atmospheric CO₂ transport based on observed winds:
398 1. Analysis of observational data. In D. H. Peterson (Ed.), *Aspects of Climate Variability in
400 the Pacific and the Western Americas* (Vol. 55, pp. 165–236). Washington, D. C.: AGU.
401 <https://doi.org/10.1029/GM055p0165>

402 Kjellström, E. (1998). A Three-Dimensional Global Model Study of Carbonyl Sulfide in the
403 Troposphere and the Lower Stratosphere. *Journal of Atmospheric Chemistry*, 29, 151–177.
404 <https://doi.org/10.1023/A:1005976511096>

405 Kourtidis, K., Kelesis, A., & Petrakakis, M. (2008). Hydrogen sulfide (H₂S) in urban ambient
406 air. *Atmospheric Environment*, 42(32), 7476–7482.
407 <https://doi.org/10.1016/j.atmosenv.2008.05.066>

408 Lana, A., Bell, T. G., Simó, R., Vallina, S. M., Ballabrera-Poy, J., Kettle, A. J., et al. (2011). An
409 updated climatology of surface dimethylsulfide concentrations and emission fluxes in the
410 global ocean. *Global Biogeochemical Cycles*, 25(1). <https://doi.org/10.1029/2010GB003850>

411 Legrand, M. (1997). Ice-core records of atmospheric sulphur. *Philosophical Transactions of the
412 Royal Society of London*, 352, 241–250. <https://doi.org/10.1098/rstb.1997.0019>

413 Legrand, M., Hammer, C., de Angelis, M., Savarino, J., Delmas, R., Clausen, H., & Johnsen, S.
414 J. (1997). Sulfur-containing species (methanesulfonate and SO₄) over the last climatic cycle
415 in the Greenland Ice Core Project (central Greenland) ice core. *Journal of Geophysical
416 Research: Oceans*, 102(C12), 26663–26679. <https://doi.org/10.1029/97JC01436>

417 Mungall, E. L., Croft, B., Lizotte, M., Thomas, J. L., Murphy, J. G., Levasseur, M., et al. (2016).
418 Dimethyl sulfide in the summertime Arctic atmosphere: Measurements and source
419 sensitivity simulations. *Atmospheric Chemistry and Physics*, 16(11), 6665–6680.
420 <https://doi.org/10.5194/acp-16-6665-2016>

421 Newhall, C., Self, S., & Robock, A. (2018). Anticipating future Volcanic Explosivity Index
422 (VEI) 7 eruptions and their chilling impacts. *Geosphere*, 14(2), 572–603.
423 <https://doi.org/10.1130/GES01513.1>

424 Osman, M. B., Das, S. B., Trusel, L. D., Evans, M. J., Fischer, H., Grieman, M. M., et al. (2019).
425 Industrial-era decline in subarctic Atlantic productivity. *Nature*, 569(7757), 551–555.
426 <https://doi.org/10.1038/s41586-019-1181-8>

427 Pataki, D. E., Ehleringer, J. R., Flanagan, L. B., Yakir, D., Bowling, D. R., Still, C. J., et al.
428 (2003). The application and interpretation of Keeling plots in terrestrial carbon cycle
429 research. *Global Biogeochemical Cycles*, 17(1). <https://doi.org/10.1029/2001GB001850>

430 Patris, N., Delmas, R. J., & Jouzel, J. (2000). Isotopic signatures of sulfur in shallow Antarctic
431 ice cores. *Journal of Geophysical Research Atmospheres*, 105(D6), 7071–7078.
432 <https://doi.org/10.1029/1999JD900974>

433 Patris, N., Delmas, R. J., Legrand, M., de Angelis, M., Ferron, F. A., Stiévenard, M., & Jouzel, J.
434 (2002). First sulfur isotope measurements in central Greenland ice cores along the
435 preindustrial and industrial periods. *Journal of Geophysical Research: Atmospheres*,
436 107(11). <https://doi.org/10.1029/2001jd000672>

437 Pham, M., Miiller, J., Brasseur, G. P., & Granier, C. (1995). A three-dimensional study of the
 438 tropospheric sulfur cycle. *Journal of Geophysical Research*, 100(D12), 61–87.
 439 <https://doi.org/10.1029/95JD02095>

440 Rantanen, M., Karpechko, A. Y., Lippinen, A., Nordling, K., Hyvärinen, O., Ruosteenoja, K., et
 441 al. (2022). The Arctic has warmed nearly four times faster than the globe since 1979.
 442 *Communications Earth and Environment*, 3(1). <https://doi.org/10.1038/s43247-022-00498-3>

443 Shindell, D. T., Lamarque, J. F., Schulz, M., Flanner, M., Jiao, C., Chin, M., et al. (2013).
 444 Radiative forcing in the ACCMIP historical and future climate simulations. *Atmospheric
 445 Chemistry and Physics*, 13(6), 2939–2974. <https://doi.org/10.5194/acp-13-2939-2013>

446 Szopa, S., Naik, V., Adhikary, B., Artaxo, P., Berntsen, T., Collins, W. D., et al. (2021). Short-
 447 Lived Climate Forcers. In *Climate Change 2021: The Physical Science Basis. Contribution
 448 of Working Group I to the Sixth Assessment Report of the Intergovernmental Panel on
 449 Climate Change* (pp. 817–922). New York, NY: Cambridge University Press.
 450 <https://doi.org/10.1017/9781009157896.008>

451 Takahashi, K., Sahoo, Y. V., Nakai, Y., Motoyama, H., & Motizuki, Y. (2022). Annually
 452 Resolved Profiles of $\delta^{34}\text{S}$ and Sulfate in Shallow Ice Core DF01 (Dome Fuji, Antarctica)
 453 Spanning the Nineteenth Century and Their Geochemical Implications. *Journal of
 454 Geophysical Research: Atmospheres*, 127(9). <https://doi.org/10.1029/2021JD036137>

455 Twomey, S. (1967). Pollution and the Planetary Albedo. *Elsevier Atmospheric Environment*,
 456 8(12), 1251–1256. [https://doi.org/10.1016/0004-6981\(74\)90004-3](https://doi.org/10.1016/0004-6981(74)90004-3)

457 Twomey, S. (1977). The Influence of Pollution on the Shortwave Albedo of Clouds. *Journal of
 458 the Atmospheric Sciences*, 34, 1149–1152. [https://doi.org/10.1175/1520-0469\(1977\)034<1149:TIOPOT>2.0.CO;2](https://doi.org/10.1175/1520-0469(1977)034<1149:TIOPOT>2.0.CO;2)

459 Wasiuta, V., Norman, A.-L., & Marshall, S. (2006). Spatial patterns and seasonal variation of
 460 snowpack sulphate isotopes of the Prince of Wales Icefield, Ellesmere Island, Canada.
 461 *Annals of Glaciology*, 43, 390–396. <https://doi.org/10.3189/172756406781812311>

462 Watts, S. F. (2000). The mass budgets of carbonyl sulfide, dimethyl sulfide, carbon disulfide and
 463 hydrogen sulfide. *Atmospheric Environment*, 34, 761–779. [https://doi.org/10.1016/S1352-2310\(99\)00342-8](https://doi.org/10.1016/S1352-2310(99)00342-8)

464 Zhai, S., Wang, X., McConnell, J. R., Geng, L., Cole-Dai, J., Sigl, M., et al. (2021).
 465 Anthropogenic Impacts on Tropospheric Reactive Chlorine Since the Preindustrial.
 466 *Geophysical Research Letters*, 48(14). <https://doi.org/10.1029/2021GL093808>

467

468

469

470

471

472

473 References from SI

474 Aiuppa, A., Inguaggiato, S., McGonigle, A. J. S., O'Dwyer, M., Oppenheimer, C., Padgett, M.
 475 J., et al. (2005). H₂S fluxes from Mt. Etna, Stromboli, and Vulcano (Italy) and implications
 476 for the sulfur budget at volcanoes. *Geochimica et Cosmochimica Acta*, 69(7), 1861–1871.
 477 <https://doi.org/10.1016/j.gca.2004.09.018>

478 Alexander, B., Thiemens, M. H., Farquhar, J., Kaufman, A. J., Savarino, J., & Delmas, R. J.
 479 (2003). East Antarctic ice core sulfur isotope measurements over a complete glacial-
 480 interglacial cycle. *Journal of Geophysical Research: Atmospheres*, 108(24).
 481 <https://doi.org/10.1029/2003jd003513>

482 Alexander, Becky, Park, R. J., Jacob, D. J., & Gong, S. (2009). Transition metal-catalyzed
483 oxidation of atmospheric sulfur: Global implications for the sulfur budget. *Journal of*
484 *Geophysical Research Atmospheres*, 114(2). <https://doi.org/10.1029/2008JD010486>

485 Allard, P, Maiorani, A., Tedesco C', D., Cortecchi, G., & Turi, B. (1991). *Isotopic study of the*
486 *origin of sulfur and carbon in Solfatara fumaroles, Campi Flegrei caldera. Journal of*
487 *Volcanology and Geothermal Research* (Vol. 48).

488 Allard, Patrick. (1980). Caracteristiques geochemiques dex volatils emis par l'eruption
489 volcanique de novembre 1978 dans le rift d'Asal. *Bull. Soc. Géol. France*, 7, 825–830.
490 <https://doi.org/10.2113/gssgbull.S7-XXII.6.825>

491 Alt, J. C., Shanks, W. C., & Jackson, M. C. (1993). Cycling of sulfur in subduction zones: The
492 geochemistry of sulfur in the Mariana Island Arc and back-arc trough. *Earth and Planetary*
493 *Science Letters*, 119, 477–494. [https://doi.org/10.1016/0012-821X\(93\)90057-G](https://doi.org/10.1016/0012-821X(93)90057-G)

494 Amrani, A., Said-Ahmad, W., Shaked, Y., & Kiene, R. P. (2013). Sulfur isotope homogeneity of
495 oceanic DMSP and DMS. *Proceedings of the National Academy of Sciences of the United*
496 *States of America*, 110(46), 18413–18418. <https://doi.org/10.1073/pnas.1312956110>

497 Angleton, G. M., & Bonham, C. D. (1995). Least Squares Regression vs. Geometric Mean
498 Regression for Ecotoxicology Studies. *Applied Mathematics and Computation*, 72, 21–32.
499 [https://doi.org/10.1016/0096-3003\(94\)00161-V](https://doi.org/10.1016/0096-3003(94)00161-V)

500 Armienta, M. A., de la Cruz-Reyna, S., Soler, A., Cruz, O., Ceniceros, N., & Aguayo, A. (2010).
501 Chemistry of ash-leachates to monitor volcanic activity: An application to Popocatépetl
502 volcano, central Mexico. *Applied Geochemistry*, 25(8), 1198–1205.
503 <https://doi.org/10.1016/j.apgeochem.2010.05.005>

504 Barry, P. H., Hilton, D. R., Füri, E., Halldórsson, S. A., & Grönvold, K. (2014). Carbon isotope
505 and abundance systematics of Icelandic geothermal gases, fluids and subglacial basalts with
506 implications for mantle plume-related CO₂ fluxes. *Geochimica et Cosmochimica Acta*, 134,
507 74–99. <https://doi.org/10.1016/j.gca.2014.02.038>

508 Bindeman, I. N., Eiler, J. M., Wing, B. A., & Farquhar, J. (2007). Rare sulfur and triple oxygen
509 isotope geochemistry of volcanogenic sulfate aerosols. *Geochimica et Cosmochimica Acta*,
510 71(9), 2326–2343. <https://doi.org/10.1016/j.gca.2007.01.026>

511 Borisov, O. G. (1970). Source of native volcanogenic sulphur. *Ceokhimiya*, 963, 332–343.

512 Böttcher, M. E., Brumsack, H. J., & Dürselen, C. D. (2007). The isotopic composition of modern
513 seawater sulfate: I. Coastal waters with special regard to the North Sea. *Journal of Marine*
514 *Systems*, 67(1–2), 73–82. <https://doi.org/10.1016/j.jmarsys.2006.09.006>

515 Burke, A., Moore, K. A., Sigl, M., Nita, D. C., McConnell, J. R., & Adkins, J. F. (2019).
516 Stratospheric eruptions from tropical and extra-tropical volcanoes constrained using high-
517 resolution sulfur isotopes in ice cores. *Earth and Planetary Science Letters*, 521, 113–119.
518 <https://doi.org/10.1016/j.epsl.2019.06.006>

519 Burkholder, J. B., & et al. (2015). Chemical Kinetics and Photochemical Data for Use in
520 Atmospheric Studies. *JPL Publication 15, Evaluation No. 18*.

521 Calhoun, J. A., Bates, T. S., & Charlson, R. J. (1991). Sulfur isotope measurements of
522 submicrometer sulfate aerosol particles over the Pacific Ocean. *Geophysical Research*
523 *Letters*, 18(10), 1877–1880. <https://doi.org/10.1029/91GL02304>

524 Carn, S. A., Yang, K., Prata, A. J., & Krotkov, N. A. (2015). Extending the long-term record of
525 volcanic SO₂ emissions with the Ozone Mapping and Profiler Suite nadir mapper.
526 *Geophysical Research Letters*, 42(3), 925–932. <https://doi.org/10.1002/2014GL062437>

527 Carn, S. A., Fioletov, V. E., McLinden, C. A., Li, C., & Krotkov, N. A. (2017). A decade of
528 global volcanic SO₂ emissions measured from space. *Scientific Reports*, 7.
529 <https://doi.org/10.1038/srep44095>

530 Carnat, G., Said-Ahmad, W., Fripiat, F., Wittek, B., Tison, J. L., Uhlig, C., & Amrani, A. (2018).
531 Variability in sulfur isotope composition suggests unique dimethylsulfoniopropionate cycling
532 and microalgae metabolism in Antarctic sea ice. *Communications Biology*, 1(1).
533 <https://doi.org/10.1038/s42003-018-0228-y>

534 Chatfield, R. J., & Crutzen, P. J. (1990). Are there interactions of iodine and sulfur species in
535 marine air photochemistry? *Journal of Geophysical Research*, 95, 22319–22341.

536 Chen, Q., Schmidt, J. A., Shah, V., Jaeglé, L., Sherwen, T., & Alexander, B. (2017). Sulfate
537 production by reactive bromine: Implications for the global sulfur and reactive bromine
538 budgets. *Geophysical Research Letters*, 44(13), 7069–7078.
539 <https://doi.org/10.1002/2017GL073812>

540 Chen, Qianjie, Sherwen, T., Evans, M., & Alexander, B. (2018). DMS oxidation and sulfur
541 aerosol formation in the marine troposphere: A focus on reactive halogen and multiphase
542 chemistry. *Atmospheric Chemistry and Physics*, 18(18), 13617–13637.
543 <https://doi.org/10.5194/acp-18-13617-2018>

544 Chin, M., Jacob, D. J., Gardner, G. M., Foreman-Fowler, M. S., Spiro, P. A., & Savoie, D. L.
545 (1996). A global three-dimensional model of tropospheric sulfate. *Journal of Geophysical
546 Research Atmospheres*, 101(13), 18667–18690. <https://doi.org/10.1029/96jd01221>

547 Cole-Dai, J., Budner, D. M., & Ferris, D. G. (2006). High speed, high resolution, and continuous
548 chemical analysis of ice cores using a melter and ion chromatography. *Environmental
549 Science and Technology*, 40(21), 6764–6769. <https://doi.org/10.1021/es061188a>

550 Cole-Dai, J., Ferris, D. G., Lanciki, A. L., Savarino, J., Thiemens, M. H., & McConnell, J. R.
551 (2013). Two likely stratospheric volcanic eruptions in the 1450s C.E. found in a bipolar,
552 subannually dated 800 year ice core record. *Journal of Geophysical Research Atmospheres*,
553 118(14), 7459–7466. <https://doi.org/10.1002/jgrd.50587>

554 Delmelle, P., Bernard, A., Kusakabe, M., Fischer, T. P., & Takano, B. (2000). Geochemistry of
555 the magmatic-hydrothermal system of Kawah Ijen volcano, East Java, Indonesia. *Journal of
556 Volcanology and Geothermal Research*, 97, 31–53. [https://doi.org/10.1016/S0377-0273\(99\)00158-4](https://doi.org/10.1016/S0377-0273(99)00158-4)

558 Diamond, M. S., Director, H. M., Eastman, R., Possner, A., & Wood, R. (2020). Substantial
559 Cloud Brightening From Shipping in Subtropical Low Clouds. *AGU Advances*, 1(1).
560 <https://doi.org/10.1029/2019av000111>

561 Fischer, T. P., Arellano, S., Carn, S., Aiuppa, A., Galle, B., Allard, P., et al. (2019). The
562 emissions of CO₂ and other volatiles from the world's subaerial volcanoes. *Scientific
563 Reports*, 9(1). <https://doi.org/10.1038/s41598-019-54682-1>

564 Fry, B., Silva, S. R., Kendall, C., & Anderson, R. K. (2002). Oxygen isotope corrections for
565 online $\delta^{34}\text{S}$ analysis. *Rapid Communications in Mass Spectrometry*, 16(9), 854–858.
566 <https://doi.org/10.1002/rcm.651>

567 Galí, M., & Simó, R. (2010). Occurrence and cycling of dimethylated sulfur compounds in the
568 Arctic during summer receding of the ice edge. *Marine Chemistry*, 122(1–4), 105–117.
569 <https://doi.org/10.1016/j.marchem.2010.07.003>

570 Galí, M., Levasseur, M., Devred, E., Simó, R., & Babin, M. (2018). Sea-surface dimethylsulfide
571 (DMS) concentration from satellite data at global and regional scales. *Biogeosciences*,
572 15(11), 3497–3519. <https://doi.org/10.5194/bg-15-3497-2018>

573 Gautier, E., Savarino, J., Hoek, J., Erbland, J., Caillon, N., Hattori, S., et al. (2019). 2600-years
574 of stratospheric volcanism through sulfate isotopes. *Nature Communications*, 10(1).
575 <https://doi.org/10.1038/s41467-019-08357-0>

576 Gautier, Elsa, Savarino, J., Erbland, J., & Farquhar, J. (2018). SO₂ Oxidation Kinetics Leave a
577 Consistent Isotopic Imprint on Volcanic Ice Core Sulfate. *Journal of Geophysical Research: Atmospheres*, 123(17), 9801–9812. <https://doi.org/10.1029/2018JD028456>

578 le Gendre, E., Martin, E., Villemant, B., Cartigny, P., & Assayag, N. (2017). A simple and
579 reliable anion-exchange resin method for sulfate extraction and purification suitable for
580 multiple O- and S-isotope measurements. *Rapid Communications in Mass Spectrometry*,
581 31(1), 137–144. <https://doi.org/10.1002/rcm.7771>

582 Ghahremaninezhad, R., Norman, A. L., Abbatt, J. P. D., Levasseur, M., & Thomas, J. L. (2016).
583 Biogenic, anthropogenic and sea salt sulfate size-segregated aerosols in the Arctic summer.
584 *Atmospheric Chemistry and Physics*, 16(8), 5191–5202. <https://doi.org/10.5194/acp-16-5191-2016>

585 Giggenbach, W. F., & Matsuo, S. (1991). Evaluation of results from Second and Third IAVCEI
586 Field Workshops on Volcanic Gases, Mt Usu, Japan, and White Island, New Zealand.
587 *Applied Geochemistry*, 6, 125–141. [https://doi.org/10.1016/0883-2927\(91\)90024-J](https://doi.org/10.1016/0883-2927(91)90024-J)

588 Guenther, A. B., Jiang, X., Heald, C. L., Sakulyanontvittaya, T., Duhl, T., Emmons, L. K., &
589 Wang, X. (2012). The model of emissions of gases and aerosols from nature version 2.1
590 (MEGAN2.1): An extended and updated framework for modeling biogenic emissions.
591 *Geoscientific Model Development*, 5(6), 1471–1492. <https://doi.org/10.5194/gmd-5-1471-2012>

592 Gutierrez-Rodriguez, A., Pillet, L., Biard, T., Said-Ahmad, W., Amrani, A., Simó, R., & Not, F.
593 (2017). Dimethylated sulfur compounds in symbiotic protists: A potentially significant
594 source for marine DMS(P). *Limnology and Oceanography*, 62(3), 1139–1154.
595 <https://doi.org/10.1002/limo.10491>

596 Halmer, M. M., Schmincke, H.-U., & Graf, H.-F. (2002). The annual volcanic gas input into the
597 atmosphere, in particular into the stratosphere: a global data set for the past 100 years.
598 *Journal of Volcanology and Geothermal Research*, 115, 511–528.
599 [https://doi.org/10.1016/S0377-0273\(01\)00318-3](https://doi.org/10.1016/S0377-0273(01)00318-3)

600 Hattori, S., Iizuka, Y., Alexander, B., Ishino, S., Fujita, K., Zhai, S., et al. (2021). Isotopic
601 evidence for acidity-driven enhancement of sulfate formation after SO₂ emission control.
602 *Sci. Adv.*, 7(5). <https://doi.org/10.5281/zenodo.3403111>

603 Heald, C. L., Ridley, D. A., Kroll, J. H., Barrett, S. R. H., Cady-Pereira, K. E., Alvarado, M. J.,
604 & Holmes, C. D. (2014). Contrasting the direct radiative effect and direct radiative forcing of
605 aerosols. *Atmospheric Chemistry and Physics*, 14(11), 5513–5527.
606 <https://doi.org/10.5194/acp-14-5513-2014>

607 Holland, H. D. (1978). *The Chemistry of the Atmosphere and Oceans*. New York: Wiley-
608 Interscience.

609 Huang, J., & Jaeglé, L. (2017). Wintertime enhancements of sea salt aerosol in polar regions
610 consistent with a sea ice source from blowing snow. *Atmospheric Chemistry and Physics*,
611 17(5), 3699–3712. <https://doi.org/10.5194/acp-17-3699-2017>

612 Jaeglé, L., Quinn, P. K., Bates, T. S., Alexander, B., & Lin, J. T. (2011). Global distribution of
613 sea salt aerosols: New constraints from in situ and remote sensing observations. *Atmospheric
614 Chemistry and Physics*, 11(7), 3137–3157. <https://doi.org/10.5194/acp-11-3137-2011>

615

616

617

618 Kasasaku, K., Minari, T., Mukai, H., & Murano, K. (1999). Stable sulfur isotope ratios of the
619 gases from Mt. Sakurajima and Satsuma-Iwojima volcanoes - Assessment of volcanic sulfur
620 on rainfall sulfate in Kagoshima Prefecture . *Nippon Kagaku Kaishi* , (7), 479–486.
621 <https://doi.org/10.2165/00003495-199141040-00008>

622 Kay, J. E., & Gettelman, A. (2009). Cloud influence on and response to seasonal Arctic sea ice
623 loss. *Journal of Geophysical Research Atmospheres*, 114(18).
624 <https://doi.org/10.1029/2009JD011773>

625 Kettle, A. J., Andreae, M. O., Amouroux, D., Andreae, T. W., Bates, T. S., Berresheim, H., et al.
626 (1999). A global database of sea surface dimethylsulfide (DMS) measurements and a
627 procedure to predict sea surface DMS as a function of latitude, longitude, and month. *Global*
628 *Biogeochemical Cycles*, 13(2), 399–444. <https://doi.org/10.1029/1999GB900004>

629 Krouse, H. R., & Grinenko, V. A. (1991). Stable Isotopes: Natural and Anthropogenic. In
630 *Sulphur in the Environment* (Vol. SCOPE 43). Chichester: J. Wiley and Sons.

631 Labidi, J., Cartigny, P., Birck, J. L., Assayag, N., & Bourrand, J. J. (2012). Determination of
632 multiple sulfur isotopes in glasses: A reappraisal of the MORB δ 34S. *Chemical Geology*,
633 334, 189–198. <https://doi.org/10.1016/j.chemgeo.2012.10.028>

634 Labidi, J., Cartigny, P., & Moreira, M. (2013). Non-chondritic sulphur isotope composition of
635 the terrestrial mantle. *Nature*, 501(7466), 208–211. <https://doi.org/10.1038/nature12490>

636 Lana, A., Bell, T. G., Simó, R., Vallina, S. M., Ballabrera-Poy, J., Kettle, A. J., et al. (2011). An
637 updated climatology of surface dimethylsulfide concentrations and emission fluxes in the
638 global ocean. *Global Biogeochemical Cycles*, 25(1). <https://doi.org/10.1029/2010GB003850>

639 Latimer, R. N. C., & Martin, R. v. (2019). Interpretation of measured aerosol mass scattering
640 efficiency over North America using a chemical transport model. *Atmospheric Chemistry and*
641 *Physics*, 19(4), 2635–2653. <https://doi.org/10.5194/acp-19-2635-2019>

642 Laws, E. (1997). *Mathematical Methods for Oceanographers*. New York: John Wiley.

643 Leck, C., & Persson, C. (1996). The central Arctic Ocean as a source of dimethyl sulfide
644 Seasonal variability in relation to biological activity. *Tellus, Series B: Chemical and Physical*
645 *Meteorology*, 48(2), 156–177. <https://doi.org/10.3402/tellusb.v48i2.15834>

646 Lewicki, J. L., Fischer, T., & Williams, S. N. (2000). Chemical and isotopic compositions of
647 fluids at Cumbal Volcano, Colombia: Evidence for magmatic contribution. *Bulletin of*
648 *Volcanology*, 62(4–5), 347–361. <https://doi.org/10.1007/s004450000100>

649 Li, J., Michalski, G., Davy, P., Harvey, M., Katzman, T., & Wilkins, B. (2018). Investigating
650 Source Contributions of Size-Aggregated Aerosols Collected in Southern Ocean and Baring
651 Head, New Zealand Using Sulfur Isotopes. *Geophysical Research Letters*, 45(8), 3717–3727.
652 <https://doi.org/10.1002/2018GL077353>

653 Li, S., & Barrie, L. A. (1993). Biogenic Sulfur Aerosol in the Arctic Troposphere: 1.
654 Contributions to Total Sulfate. *Journal of Geophysical Research*, 98, 613–633.
655 <https://doi.org/10.1029/93JD02234>

656 Lin, C. T., Baker, A. R., Jickells, T. D., Kelly, S., & Lesworth, T. (2012). An assessment of the
657 significance of sulphate sources over the Atlantic Ocean based on sulphur isotope data.
658 *Atmospheric Environment*, 62, 615–621. <https://doi.org/10.1016/j.atmosenv.2012.08.052>

659 Liotta, M., Rizzo, A., Paonita, A., Caracausi, A., & Martelli, M. (2012). Sulfur isotopic
660 compositions of fumarolic and plume gases at Mount Etna (Italy) and inferences on their
661 magmatic source. *Geochemistry, Geophysics, Geosystems*, 13(5).
662 <https://doi.org/10.1029/2012GC004118>

663 Loeb, N. G., Doelling, D. R., Wang, H., Su, W., Nguyen, C., Corbett, J. G., et al. (2018). Clouds
664 and the Earth'S Radiant Energy System (CERES) Energy Balanced and Filled (EBAF) top-
665 of-atmosphere (TOA) edition-4.0 data product. *Journal of Climate*, 31(2), 895–918.
666 <https://doi.org/10.1175/JCLI-D-17-0208.1>

667 Longhurst, A. (1998). *Ecological Geography of the Sea*. Academic Press.

668 Loose, B., McGillis, W. R., Schlosser, P., Perovich, D., & Takahashi, T. (2009). Effects of
669 freezing, growth, and ice cover on gas transport processes in laboratory seawater
670 experiments. *Geophysical Research Letters*, 36(5). <https://doi.org/10.1029/2008GL036318>

671 Marini, L., Gambardella, B., Principe, C., Arias, A., Brombach, T., & Hunziker, J. C. (2000).
672 Characterization of magmatic sulfur in the Aegean island arc by means of the d34S values of
673 fumarolic H2S, elemental S, and hydrothermal gypsum from Nisyros and Milos islands.
674 *Earth and Planetary Science Letters*, 200, 15–31. [https://doi.org/10.1016/S0012-821X\(02\)00611-8](https://doi.org/10.1016/S0012-821X(02)00611-8)

675 Martin, E., Bekki, S., Ninin, C., & Bindeman, I. (2014). Volcanic sulfate aerosol formation in the
676 troposphere. *Journal of Geophysical Research Atmospheres*, 119(22), 12,660-12,673.
677 <https://doi.org/10.1002/2014JD021915>

678 Martin, R. S., Roberts, T. J., Mather, T. A., & Pyle, D. M. (2009). The implications of H2S and
679 H2 kinetic stability in high-T mixtures of magmatic and atmospheric gases for the production
680 of oxidized trace species (e.g., BrO and NOx). *Chemical Geology*, 263(1–4), 143–150.
681 <https://doi.org/10.1016/j.chemgeo.2008.12.028>

682 Mather, T. A., McCabe, J. R., Rai, V. K., Thiemens, M. H., Pyle, D. M., Heaton, T. H. E., et al.
683 (2006). Oxygen and sulfur isotopic composition of volcanic sulfate aerosol at the point of
684 emission. *Journal of Geophysical Research Atmospheres*, 111(18).
685 <https://doi.org/10.1029/2005JD006584>

686 Matrai, P. A. (1997). Dynamics of the vernal bloom in the marginal ice zone of the Barents Sea:
687 Dimethyl sulfide and dimethylsulfoniopropionate budgets. *Journal of Geophysical Research
688 C: Oceans*, 102(C10), 22965–22979. <https://doi.org/10.1029/96JC03870>

689 McCoy, D. T., Bender, F. A. M., Grosvenor, D. P., Mohrmann, J. K., Hartmann, D. L., Wood,
690 R., & Field, P. R. (2018). Predicting decadal trends in cloud droplet number concentration
691 using reanalysis and satellite data. *Atmospheric Chemistry and Physics*, 18(3), 2035–2047.
692 <https://doi.org/10.5194/acp-18-2035-2018>

693 McDuffie, E. E., Smith, S. J., O'Rourke, P., Tibrewal, K., Venkataraman, C., Marais, E. A., et al.
694 (2020). A global anthropogenic emission inventory of atmospheric pollutants from sector-
695 And fuel-specific sources (1970-2017): An application of the Community Emissions Data
696 System (CEDS). *Earth System Science Data*, 12(4), 3413–3442. <https://doi.org/10.5194/essd-12-3413-2020>

697 Millet, D. B., Baasandorj, M., Farmer, D. K., Thornton, J. A., Baumann, K., Brophy, P., et al.
698 (2015). A large and ubiquitous source of atmospheric formic acid. *Atmospheric Chemistry
699 and Physics*, 15(11), 6283–6304. <https://doi.org/10.5194/acp-15-6283-2015>

700 Mizutani, Y., & Sugiura, T. (1982). Variations in chemical and isotopic compositions of
701 fumarolic gases from Showashinzan volcano, Hokkaido, Japan. *Geochemical Journal*, 16(2),
702 63–71. <https://doi.org/10.2343/geochemj.16.63>

703 de Moor, J. M., Fischer, T. P., Sharp, Z. D., King, P. L., Wilke, M., Botcharnikov, R. E., et al.
704 (2013). Sulfur degassing at Erta Ale (Ethiopia) and Masaya (Nicaragua) volcanoes:
705 Implications for degassing processes and oxygen fugacities of basaltic systems.

708 *Geochemistry, Geophysics, Geosystems*, 14(10), 4076–4108.
709 <https://doi.org/10.1002/ggge.20255>

710 de Moor, J. Maarten, Fischer, T. P., Sharp, Z. D., Hauri, E. H., Hilton, D. R., & Atudorei, V.
711 (2010). Sulfur isotope fractionation during the May 2003 eruption of Anatahan volcano,
712 Mariana Islands: Implications for sulfur sources and plume processes. *Geochimica et*
713 *Cosmochimica Acta*, 74(18), 5382–5397. <https://doi.org/10.1016/j.gca.2010.06.027>

714 Mungall, E. L., Croft, B., Lizotte, M., Thomas, J. L., Murphy, J. G., Levasseur, M., et al. (2016).
715 Dimethyl sulfide in the summertime Arctic atmosphere: Measurements and source sensitivity
716 simulations. *Atmospheric Chemistry and Physics*, 16(11), 6665–6680.
717 <https://doi.org/10.5194/acp-16-6665-2016>

718 Nielsen, H., Pilot, J., Grinenko, L. N., Grinenko, V. A., Lein, A. Y., Smith, J. W., & Pankina, R.
719 G. (1991). *Lithospheric Sources of Sulphur*. (H. R. Krouse & V. A. Grinenko, Eds.), *Stable*
720 *Isotopes: Natural and Anthropogenic Sulphur in the Environment*. New York: John Wiley.

721 Norman, A. L., Barrie, L. A., Toom-Sauntry, D., Sirois, A., Krouse, H. R., Li, S. M., & Sharma,
722 S. (1999). Sources of aerosol sulphate at Alert: apportionment using stable isotopes. *Journal*
723 *of Geophysical Research*, 104(D9), 11,619–11,631. <https://doi.org/10.1029/1999JD900078>

724 Norman, A. L., Belzer, W., & Barrie, L. (2004). Insights into the biogenic contribution to total
725 sulphate in aerosol and precipitation in the Fraser Valley afforded by isotopes of sulphur and
726 oxygen. *Journal of Geophysical Research: Atmospheres*, 109(5).
727 <https://doi.org/10.1029/2002jd003072>

728 Novak, G. A., Fite, C. H., Holmes, C. D., Veres, P. R., Neuman, J. A., Faloona, I., et al. (2021).
729 Rapid cloud removal of dimethyl sulfide oxidation products limits SO₂ and cloud
730 condensation nuclei production in the marine atmosphere. *Proceedings of the National*
731 *Academy of Sciences*, 118(42), e2110472118. <https://doi.org/10.1073/pnas.2110472118/-/DCSupplemental>

732 Nriagu, J. O., & Coker, R. D. (1978). Isotopic composition of sulfur in precipitation within the
733 Great Lakes Basin. *Tellus*, 30, 365–375. <https://doi.org/10.1111/j.2153-3490.1978.tb00852.x>

734 Oduro, H., van Alstyne, K. L., & Farquhar, J. (2012). Sulfur isotope variability of oceanic DMSP
735 generation and its contributions to marine biogenic sulfur emissions. *Proceedings of the*
736 *National Academy of Sciences of the United States of America*, 109(23), 9012–9016.
737 <https://doi.org/10.1073/pnas.1117691109>

738 Park, R. J. (2004). Natural and transboundary pollution influences on sulfate-nitrate-ammonium
739 aerosols in the United States: Implications for policy. *Journal of Geophysical Research*,
740 109(D15). <https://doi.org/10.1029/2003jd004473>

741 Pataki, D. E., Ehleringer, J. R., Flanagan, L. B., Yakir, D., Bowling, D. R., Still, C. J., et al.
742 (2003). The application and interpretation of Keeling plots in terrestrial carbon cycle
743 research. *Global Biogeochemical Cycles*, 17(1). <https://doi.org/10.1029/2001GB001850>

744 Patris, N., Delmas, R. J., & Jouzel, J. (2000). Isotopic signatures of sulfur in shallow Antarctic
745 ice cores. *Journal of Geophysical Research Atmospheres*, 105(D6), 7071–7078.
746 <https://doi.org/10.1029/1999JD900974>

747 Patris, N., Delmas, R. J., Legrand, M., de Angelis, M., Ferron, F. A., Stiévenard, M., & Jouzel, J.
748 (2002). First sulfur isotope measurements in central Greenland ice cores along the
749 preindustrial and industrial periods. *Journal of Geophysical Research: Atmospheres*, 107(11).
750 <https://doi.org/10.1029/2001jd000672>

751 Perrette, M., Yool, A., Quartly, G. D., & Popova, E. E. (2011). Near-ubiquity of ice-edge blooms
752 in the Arctic. *Biogeosciences*, 8(2), 515–524. <https://doi.org/10.5194/bg-8-515-2011>

753

754 Rafter, T. A., Wilson, S. H., & Shilton, B. W. (1958). Sulphur isotopic measurements on the
755 discharge from fumaroles on White Island. In *Sulphur isotopic variations in nature* (Vol. 1,
756 pp. 154–171). N. J. Z. Sci.

757 Rees, C. E., Jenkins, W. J., & Monster, J. (1978). The sulphur isotopic composition of ocean
758 water sulphate*. *Geochimica et Cosmochimica Acta*, 42(4), 377–381.
759 [https://doi.org/10.1016/0016-7037\(78\)90268-5](https://doi.org/10.1016/0016-7037(78)90268-5)

760 Robinson, B. W. (1985). Sulphur and sulphate-oxygen isotopes in New Zealand geothermal
761 systems and volcanic discharges. In *Studies on sulphur isotope variations in nature* (pp. 31–
762 48). Vienna: International Atomic Energy Agency.

763 Rye, R. O., Luhr, J. F., & Wasserman, M. D. (1984). Sulfur and oxygen isotopic systematics of
764 the 1982 eruptions of El Chichón Volcano. *J. Volcanol. Geotherm. Res.*, 23, 109–123.
765 [https://doi.org/10.1016/0377-0273\(84\)90058-1](https://doi.org/10.1016/0377-0273(84)90058-1)

766 Sakai, H., & Nagasawa, H. (1958). Fractionation of sulphur isotopes in volcanic gases.
767 *Geochimica et Cosmochimica Acta*, 15, 32–39. [https://doi.org/10.1016/0016-7037\(58\)90007-3](https://doi.org/10.1016/0016-7037(58)90007-3)

769 Sakai, Hitoshi. (1957). Fractionation of sulphur isotopes in nature. *Geochimica et Cosmochimica
770 Acta*, 12(1–2), 160–169.

771 Sakai, Hitoshi, Casadevall, T. J., & Moore, J. G. (1982). Chemistry and isotope ratios of sulfur in
772 basalts and volcanic gases at Kilauea Volcano, Hawaii. *Geochimica et Cosmochimica Acta*,
773 46, 729–738. [https://doi.org/10.1016/0016-7037\(82\)90024-2](https://doi.org/10.1016/0016-7037(82)90024-2)

774 Sanusi, A. A., Norman, A. L., Burridge, C., Wadleigh, M., & Tang, W. W. (2006).
775 Determination of the S isotope composition of methanesulfonic acid. *Analytical Chemistry*,
776 78(14), 4964–4968. <https://doi.org/10.1021/ac0600048>

777 Sharma, S., Chan, E., Ishizawa, M., Toom-Sauntry, D., Gong, S. L., Li, S. M., et al. (2012).
778 Influence of transport and ocean ice extent on biogenic aerosol sulfur in the Arctic
779 atmosphere. *Journal of Geophysical Research Atmospheres*, 117(12).
780 <https://doi.org/10.1029/2011JD017074>

781 Shindell, D. T., Lamarque, J. F., Schulz, M., Flanner, M., Jiao, C., Chin, M., et al. (2013).
782 Radiative forcing in the ACCMIP historical and future climate simulations. *Atmospheric
783 Chemistry and Physics*, 13(6), 2939–2974. <https://doi.org/10.5194/acp-13-2939-2013>

784 Siegel, K., Karlsson, L., Zieger, P., Baccarini, A., Schmale, J., Lawler, M., et al. (2021). Insights
785 into the molecular composition of semi-volatile aerosols in the summertime central Arctic
786 Ocean using FIGAERO-CIMS. *Environmental Science: Atmospheres*, 1(4), 161–175.
787 <https://doi.org/10.1039/d0ea00023j>

788 Stjern, C. W., Muri, H., Ahlm, L., Boucher, O., Cole, J. N. S., Ji, D., et al. (2018). Response to
789 marine cloud brightening in a multi-model ensemble. *Atmospheric Chemistry and Physics*,
790 18(2), 621–634. <https://doi.org/10.5194/acp-18-621-2018>

791 Symonds, R. B., Janik, C. J., Evans, W. C., Ritchie, B. E., Counce, D., Poreda, R. J., & Iven, M.
792 (2003). Scrubbing Masks Magmatic Degassing During Repose at Cascade-Range and
793 Aleutian-Arc Volcanoes. *US Geological Survey Open-File Report*, 03(435).

794 Tian, L., & Curry, J. A. (1989). Cloud Overlap Statistics 1 2. *Journal of Geophysical Research*,
795 94(D7), 9,925–9,935.

796 Torssander, P. (1988). Sulfur isotope ratios of Icelandic lava incrustations and volcanic gases.
797 *Journal of Volcanology and Geothermal Research*, 35, 227–235.
798 [https://doi.org/10.1016/0377-0273\(88\)90019-4](https://doi.org/10.1016/0377-0273(88)90019-4)

799 Vinogradov, V. I. (1980). Isotopic composition of elements and the problem of mantle
800 degassification and the formation of the gas-water cover of the Earth. *Degazatsiya Zemli i*
801 *Geotektonika*, 1, 23–30.

802 Wadleigh, M. A. (2004). Sulphur isotopic composition of aerosols over the western North
803 Atlantic Ocean. In *Canadian Journal of Fisheries and Aquatic Sciences* (Vol. 61, pp. 817–
804 825). <https://doi.org/10.1139/F04-073>

805 Wang, X., Jacob, D. J., Eastham, S. D., Sulprizio, M. P., Zhu, L., Chen, Q., et al. (2019). The
806 role of chlorine in global tropospheric chemistry. *Atmospheric Chemistry and Physics*, 19(6),
807 3981–4003. <https://doi.org/10.5194/acp-19-3981-2019>

808 Wasiuta, V., Norman, A.-L., & Marshall, S. (2006). Spatial patterns and seasonal variation of
809 snowpack sulphate isotopes of the Prince of Wales Icefield, Ellesmere Island, Canada.
810 *Annals of Glaciology*, 43, 390–396. <https://doi.org/10.3189/172756406781812311>

811 Wasserman, L. (2004). The Bootstrap. In *All of Statistics* (pp. 107–118). Springer
812 Science+Business Media. https://doi.org/10.1007/978-0-387-21736-9_8

813 Watts, S. F. (2000). The mass budgets of carbonyl sulfide, dimethyl sulfide, carbon disulfide and
814 hydrogen sulfide. *Atmospheric Environment*, 34, 761–779. [https://doi.org/10.1016/S1352-2310\(99\)00342-8](https://doi.org/10.1016/S1352-
815 2310(99)00342-8)

816 Webb, M. J., Andrews, T., Bodas-Salcedo, A., Bony, S., Bretherton, C. S., Chadwick, R., et al.
817 (2017). The Cloud Feedback Model Intercomparison Project (CFMIP) contribution to
818 CMIP6. *Geoscientific Model Development*, 10(1), 359–384. [https://doi.org/10.5194/gmd-10-359-2017](https://doi.org/10.5194/gmd-10-
819 359-2017)

820 Williams, S. N., Sturchio, N. C., Calvache V., M. L., Mendez F., R., Londoño C., A., & García
821 P., N. (1990). Sulfur dioxide from Nevado del Ruiz volcano, Colombia: total flux and
822 isotopic constraints on its origin. *Journal of Volcanology and Geothermal Research*, 42(1–2),
823 53–68.

824 Wood, R. (2021). Assessing the potential efficacy of marine cloud brightening for cooling Earth
825 using a simple heuristic model. *Atmospheric Chemistry and Physics*, 21(19), 14507–14533.
826 <https://doi.org/10.5194/acp-21-14507-2021>

827 Zemmelink, H. J., Dacey, J. W. H., Houghton, L., Hintsa, E. J., & Liss, P. S. (2008).
828 Dimethylsulfide emissions over the multi-year ice of the western Weddell Sea. *Geophysical
829 Research Letters*, 35(6). <https://doi.org/10.1029/2007GL031847>

830

831